Charge-state dependence of binary-encounter-electron cross sections and peak energies

H. I. Hidmi, P. Richard, J. M. Sanders,* H. Schöne,† J. P. Giese, D. H. Lee,‡ T. J. M. Zouros,§ and S. L. Varghese‖

J. R. Macdonald Laboratory, Department of Physics, Kansas State University, Manhattan, Kansas 66506

(Received 24 November 1992; revised manuscript received 15 July 1993)

The charge-state dependence of the binary-encounter-electron (BEE) double-differential cross section (DDCS) at 0° with respect to the beam direction resulting from collisions of 1 MeV/amu H^+, C^{q+}, N^{q+}, O^{q+}, F^{q+}, Si^{q+}, and Cl^{q+}, and 0.5 MeV/amu Cu^{q+} with H_2 is reported. The data show an enhancement in the BEE DDCS as the charge state of the projectile is decreased, in agreement with the data reported by Richard *et al.* [J. Phys. B **23**, L213 (1990)]. The DDCS enhancement ratios observed for the three-electron isoelectronic sequence C^{3+}:C^{6+}, N^{4+}:N^{7+}, O^{5+}:O^{8+}, and F^{6+}:F^{9+} are about 1.35, whereas a DDCS enhancement of 3.5 was observed for Cu^{4+}. The BEE enhancement with increasing electrons on the projectile has been shown by several authors to be due to the non-Coulomb static potential of the projectile and additionally to the *e-e* exchange interaction. An impulse-approximation (IA) model fits the shape of the BEE DDCS and predicts a Z_p^2 dependence for the bare-ion cross sections. The IA also predicts a binary peak energy that is independent of q and Z_p and below the classical value of $4t$, where t is the energy of electrons traveling with the projectile velocity. We observed a BEE energy shift ΔE (ΔE=$4t - E_{\rm peak}$, where $E_{\rm peak}$ is the measured energy at the peak of the binary encounter electrons) that is approximately independent of q for the low-Z_p ions, whereas the measured ΔE values for Si, Cl, and Cu were found to be q dependent.

PACS number(s): 34.70.+e

I. INTRODUCTION

In the collision between a heavy-ion projectile and a target, electrons with widely different energies are emitted from the collision [1]. Target electrons may be ionized and ejected with low energy when the impact parameter of the collision is large. Electrons captured by the projectile to the continuum (ECC), or lost by the projectile to the continuum (ELC), are called cusp electrons and are characterized by having a velocity equal to the velocity of the projectile. Target electrons may be ionized by the projectile as a result of a collision at a very small target electron-projectile impact parameter and these electrons are referred to as binary-encounter electrons (BEE's) and are emitted with high velocity. Figure 1 gives a typical spectrum observed at zero degrees in the laboratory frame for a heavy projectile on an H_2 target where the cusp and BEE features are identified.

This paper deals with the production of the binary encounter electrons, which are target electrons ionized through direct, hard collisions with energetic projectiles. The ionized electrons have a broad energy spectrum due to their momentum distribution in the target. Based on classical two-body collision dynamics for heavy-ion impact on a *free* electron, the energy of the recoiling elec-

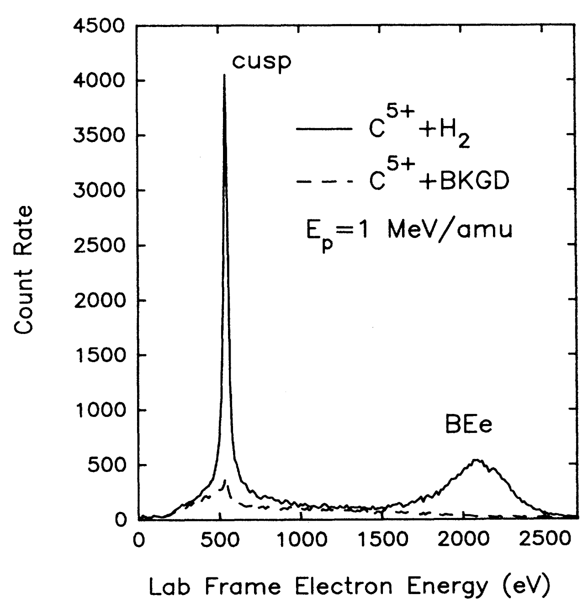

FIG. 1. Electron count rate as a function of laboratory-frame electron energy for 1 MeV/amu C^{5+} projectiles with H_2 gas in the gas cell (solid line) and without H_2 gas in the gas cell (dashed line).

*Present address: Oak Ridge National Laboratory, Bldg. 5500, MS-6377, Oak Ridge, TN 37831.

†Present address: Sandia National Laboratories, Albuquerque, NM 87185.

‡Present address: Oak Ridge National Laboratory, Bldg. 5500, P.O. Box 2008, Oak Ridge, TN 37831.

§Present address: Department of Physics, University of Crete and Institute of Electronic Structure and Laser, P. O. Box 1527, Heraklion 711 10, Crete, Greece.

‖Present address: Department of Physics, University of South Alabama, Mobile, AL 36688.

tron can be shown to equal $4t\cos^2\theta_{\rm lab}$. The cusp-electron energy is given by $t=(m_e/M_p)E_p$, where m_e is the electron mass, M_p is the projectile mass, E_p is the projectile energy, and $\theta_{\rm lab}$ is the laboratory observation angle with respect to the beam direction. For an observation angle of 0°, the BEE peak produced in a collision between an ion and a free electron should therefore be at $4t$.

In a recent paper Lee *et al.* [2] reported on the double-differential electron production cross section of BEE at an observation angle of 0° with respect to the beam direction in energetic 1–2-MeV/amu collisions of bare ions with H_2 and He targets. An impulse-approximation (IA) model describing the production process in which the quasifree target electrons undergo 180° Rutherford scattering in the projectile frame was developed. It was found that the double-differential cross sections (DDCS) for the bare ions were well described by this model and were found to scale with Z_p^2 for $Z_p \leq 9$. For nonbare projectile ions, Richard *et al.* [3] reported an enhancement of the BEE DDCS production for the case of nonbare F projectiles at an observation angle of 0° in the laboratory frame. It was found that the enhancements of the BEE yields for F^{8+} and F^{3+} relative to F^{9+} were about 15% and 50%, respectively. Kelbch *et al.* [4] and Hagmann *et al.* [5] observed a structure not characteristic of BEE production in some non 0° electron spectra involving very-heavy-ion projectiles on rare-gas targets.

Recently, Schultz and Olson [6], Shingal *et al.* [7], Chen, Madison and Lin [8], and Bhalla and Shingal [9] presented calculations of the BEE production cross sections that explain the enhancement observed by Richard *et al.* [3]. Reinhold, Schultz, and Olson [10] and Schultz and Olson [6] explain the enhancement as due to scattering from the non-Coulomb static potential of the projectile. Bhalla and Shingal [9] included the effect of both the non-Coulomb static and electron exchange potentials. Taulbjerg [11] had previously shown the importance of electron exchange in his calculation of F^{8+} on H_2.

In a recent communication, González *et al.* [12] measured the BEE enhancement ratio for hydrogenlike He, C, N, O, and F ions on H_2 relative to bare ions on H_2. They normalized their data to the data by Richard *et al.* [3] for bare F and found that the enhancement ratio compares favorably with the theory of Taulbjerg. Other papers [13–15] also have been presented which verify this enhancement.

In this paper, we report the observation of the enhancement of the binary-encounter-electron DDCS at 0° with respect to the beam direction in energetic 1 MeV/amu collisions of C^{q+}, N^{q+}, O^{q+}, F^{q+}, Si^{q+}, and Cl^{q+} on H_2, and 0.5 MeV/amu Cu^{q+} on H_2, as a function of the projectile charge state. It was possible to obtain from our accelerator the bare projectile ions at these energies only for the low Z_p ions ($Z_p < 14$). We measure in this experiment the binary-encounter peak-energy shift $\Delta E = 4t - E_{\rm peak}$ as a function of the projectile charge state q for various nuclear charges Z_p. The measured BEE peak energy shift is compared to the Bohr-Lindhard model [15] and the measured enhancements are compared to the available calculations of Schultz and Olson [6] and Bhalla and Shingal [9].

II. EXPERIMENT

The experiment was performed using highly charged ion beams produced by the tandem Van de Graaff accelerator in the J. R. Macdonald Laboratory at Kansas State University. The energies of the electrons were analyzed at 0° using a tandem 45° parallel-plate electron spectrometer [16], which was equipped with a channel electron multiplier for electron detection. The binary-encounter electrons were recorded under single-collision conditions, found to be valid for target pressures less than 80 mTorr in the 10-cm-long gas cell. The gas cell was doubly differentially pumped so that the chamber pressure could be maintained below 0.01 mTorr at typical gas cell pressures of 20 mTorr or less. A shielded Faraday cup was used to measure the beam current in order to normalize the electron count for each electron energy channel. No correction was applied to the measured beam current due to electron capture by or ionization of the projectile since these effects were found to be negligible for the collision systems studied [2].

Background counts in the electron spectra are produced mainly by electrons scattered by the beam striking the edges of the spectrometer slits and gas cell apertures as well as the residual gas, and can be a large source of error. This beam-induced electron background was directly determined by taking an electron spectrum without any gas in the target cell. Around the BEE peak, this background was found to be less than 5% of the true count and was subtracted from the electron spectrum taken with gas in the cell (see Fig. 1). In order to check if there was any contamination in the H_2 gas, the gas line was cooled with liquid nitrogen (LN_2) to freeze out heavy contaminants. Spectra were taken with and without LN_2 trapping and were found to give identical results. If such contaminants were present, the binary-encounter peak would be broader than that for H_2 targets due to the larger target electron momentum distribution in the heavy-element contaminants. Also, since the efficiency of the system is not 100%, the data were multiplied by a normalization factor which was deduced from the bare F ion case [2]. In all cases, the theory for the bare projectile ion was scaled up to fit the BEE data, and the scaling factor was used to evaluate the cross-section enhancement ratios. For some projectiles at 1 MeV/amu, the projectile Auger lines appear on top of or very close to the binary-encounter peak, which makes it difficult to extract the cross section at the peak.

For the lower charge states, the cusp was found to be very intense, very wide, and had a tail extending toward the binary-encounter peak. For these lower-charge-state cases, since the projectile has many electrons, electron loss to the continuum (ELC) is the major contributor to the cusp and to the high-energy tail. We do not attempt to account for these electrons. The beam energy E_p was determined directly from the measured cusp-electron energy. A short scan of 1 eV steps was taken around the cusp, the cusp peak energy t was then determined, and the beam energy E_p was thus obtained by the relation $E_p=(M_p/m_e)t$.

III. THEORY

The BEE production cross section for the bare ion can be evaluated in the projectile frame within the impulse approximation treatment [2,17], which is valid for collisions in which the projectile velocity is much larger than the target electron velocity, as follows:

$$\left(\frac{d\sigma}{d\Omega}\right)_{\rm BEE} = \sum_i \int \left[\frac{Z_p^2 e^4}{16E^2 \sin^4(\theta/2)}\right] |\psi_i(\mathbf{p}_i)|^2 d^3p_i. \quad (1)$$

The expression within the square brackets on the right-hand side of the equation is the Rutherford scattering cross section of a free electron by a bare projectile ion of nuclear charge Z_pe. For the 0° BEE measurement, the electron scattering angle is θ=180° in the projectile frame. The target momentum wave function is given by $\psi_i(\mathbf{p}_i)$, where the subscript i refers to the ith target electron. E is the electron energy in the projectile frame, and if the target ionization energy E_I is included, it can be written as

$$E = (\mathbf{s} + \mathbf{p}_i)^2/2m - E_I, \quad (2)$$

where $\mathbf{s}$ is the cusp momentum with a magnitude given by $s = mV_p$, and V_p is the projectile velocity. If we choose the beam direction to be along the z axis, the transverse components of the electron momentum in the projectile frame at high projectile velocity are small compared to s and can thus be neglected. The electron energy then can be written approximately as [2]

$$E = (s^2 + 2sp_{iz} + p_{iz}^2)/2m - E_I. \quad (3)$$

In terms of the Compton profile $J(p_{iz})$, which is the projection of $\psi(\mathbf{p}_i)$ on the z axis, and the Rutherford cross section $(\frac{d\sigma}{d\Omega})_{\rm Ruth}$, the DDCS may be written as

$$\left(\frac{d^2\sigma}{dEd\Omega}\right)_{\rm BEE} = \sum_i \left(\frac{d\sigma}{d\Omega}\right)_{\rm Ruth} \frac{J(p_{iz})}{(V_p + p_{iz})}. \quad (4)$$

In order to compare with theory, the experimental DDCS and electron energies are transformed from the laboratory frame to the projectile frame, using [1,18]

$$\left(\frac{d^2\sigma}{dEd\Omega}\right)_{\rm BEE} = \left(\frac{d^2\sigma}{dEd\Omega}\right)_{\rm BEE}^{\rm lab} \sqrt{E/E_{\rm lab}}, \quad (5)$$

where, for θ =180° ($\theta_{\rm lab} = 0°$),

$$\sqrt{E} = \sqrt{E_{\rm lab}} - \sqrt{t}, \quad (6)$$

where $E_{\rm lab}$ is the electron energy in the laboratory frame.

In the case of a nonbare projectile ion, the electron-electron interaction between the target electrons and the projectile electrons leads to two different effects which must be included in the elastic-scattering cross section. The first is the screening of the projectile by its electrons during the collision with the quasifree target electrons. The second is the electron exchange between a projectile electron and a target electron. Both of these effects enhance [9,11] the elastic-scattering cross section at $\theta_{\rm lab} = 0°$. A classical picture of the screening effect is that the scattered target electron is attracted by a $\frac{qe^2}{r}$ field at large distances and a $\frac{Z_pe^2}{r}$ field at small distances from the projectile nucleus. The net effect is that for a nonbare projectile ion the electron has a smaller kinetic energy than for a bare ion at small values of r but still scatters from a bare nucleus (particularly for 180° scattering). This electron, therefore, has an enhanced elastic scattering cross section due to the $\frac{1}{E^2}$ behavior of the Rutherford scattering. This enhancement effect is verified in purely classical calculations [6,19], as well as in the quantum calculations. In the calculations performed to date, the screening and exchange effects contribute approximately equally to the enhancement for the systems we have studied.

The IA model in the form of Eq. (4) can still be employed to calculate the DDCS for BEE production for nonbare projectile ions; however, the Rutherford cross section $(\frac{d\sigma}{d\Omega})_{\rm Ruth}$ must be replaced by the proper elastic scattering cross section $(\frac{d\sigma}{d\Omega})_{\rm el}$. The radial wave function of the scattered state of the incident electron is a solution of the second-order coupled integro-differential equation of the form [9]:

$$\left(\frac{d^2}{dr^2} + \frac{l(l+1)}{r^2} - 2V(r) + k^2\right)u_l(r) = X_l(r), \quad (7)$$

where l is the angular momentum of the electron, k is its linear momentum, $X_l(r)$ is the nonlocal exchange contribution, and $V(r)$ is given by

$$V(r) = \frac{-q}{r} + V_s(r), \quad (8)$$

where q is the charge state of the projectile and $V_s(r)$ is the non-Coulomb static potential. The scattering amplitude $f(\theta)$ is given by

$$f(\theta) = f_C(\theta) + f_s(\theta), \quad (9)$$

where $f_C(\theta)$ is the asymptotic Coulomb scattering amplitude and $f_s(\theta)$ is the scattering amplitude associated with $V_s(r)$. The elastic-scattering cross section is then given by

$$\left(\frac{d\sigma}{d\Omega}\right)_{\rm el} = |f_C(\theta) + f_s(\theta)|^2. \quad (10)$$

Bhalla and Shingal [9] have calculated the contribution of the non-Coulomb static potential and the contribution of the nonlocal two-electron exchange potential to the cross section in a self-consistent Hartree-Fock model using this formulation of the problem.

IV. DATA ANALYSIS

In this experiment we studied the effect of the projectile ion charge state on the BEE DDCS for different projectile ions. We also studied the BEE peak shift ΔE as a function of projectile charge state q and nuclear charge Z_p. Figure 2(a) shows the laboratory-frame DDCS for

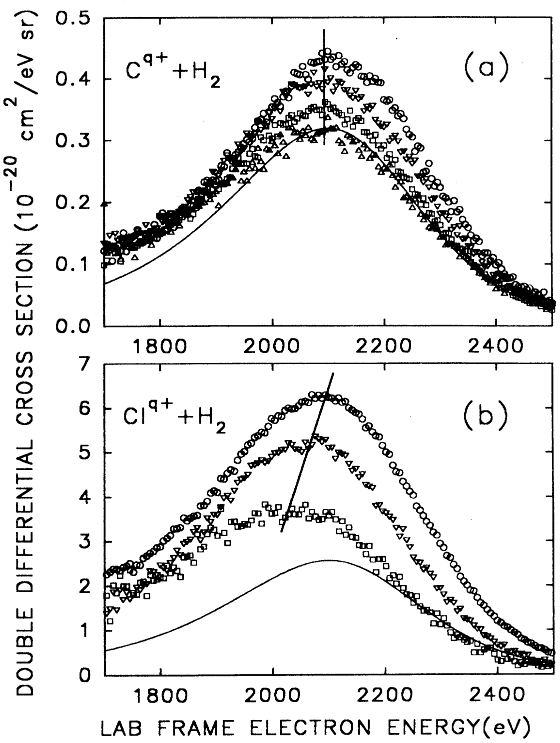

FIG. 2. (a) Absolute binary-encounter-electron double-differential cross section for 1 MeV/amu C^{q+} on H_2. Circles, q=3; down triangles, q = 4; squares, q=5; up triangles, q=6. The solid line is the theoretical calculation for the bare ion according to Eq. (4). The solid vertical line is drawn to show the position of the BEE peak as a function of q. (b) Same as (a) but for 1 MeV/amu Cl^{q+} on H_2. Circles, q=5; triangles, q=9, squares, q=13.

collisions of 1 MeV/amu C^{q+} with H_2 for four different charge states (q=3, 4, 5, and 6). Similar results were obtained for N^{q+} (q=3–7), O^{q+} (q=3-8), and F^{q+} (q=3–9). Figure 2(b) shows the laboratory-frame DDCS for collisions of 1 MeV/amu Cl^{q+} for q=5, 9, and 13. The other chlorine projectile charge states studied (q=7, 8, 10, 11, and 12) are not included in the figure for clarity. Similar results were obtained for Si^{q+} and Cu^{q+}. The solid curve in each of the two figures is the calculation of the DDCS for the bare ion using Eq. (4) above. The lines connecting the peaks are drawn to show the change in the position of the peaks as a function of q.

A. BEE enhancement

It is apparent that the BEE DDCS increases by increasing the number of electrons on the projectile for all the ions studied. This is in agreement with the data reported by Richard *et al.* [3]. Also our data are in agreement with the data reported by González *et al.* [12] for hydrogenlike ions. Table I lists the enhancement ratios $R = \sigma(q)/\sigma(Z_p)$, where $\sigma(q)$ is the BEE DDCS for the ion of charge state q and $\sigma(Z_p)$ is the BEE DDCS of the bare projectile ion [20]. Table I includes the present data as well as the available theoretical calculations of both Schultz and Olson [6] and Bhalla and Shingal [9] for carbon and fluorine. The values of the ratios for carbon and fluorine of Bhalla and Shingal [9] are slightly higher than our data, but they are in slightly better agreement with our data than the values of Schultz and Olson [6]. Schultz and Olson [6] obtained a lower value of the ratio for C than Bhalla and Shingal [9]. The inclusion of electron-electron exchange by Bhalla and Shingal [9] is the reason for the higher predicted ratios. The electron-electron exchange is predicted to have a larger effect at

TABLE I. Experimental and theoretical enhancement ratios $R = \sigma(q)/\sigma(Z_p)$ as a function of the charge state of the projectiles for 1 MeV/amu H, C, N, O, F, and Cl and 0.5 MeV/amu Cu projectile ions. $\sigma(q)$ is the double-differential cross section at the binary-encounter peak for a projectile ion of charge state q. $\sigma(Z_p)$ is the corresponding double-differential cross section for the bare projectile ion of nuclear charge Z_p.

q	R (Experiment)							R (Theory)			
	C	N	O	F	Si	Cl	Cu	C[a]	C[b]	F[a]	F[b]
3	1.34±0.05	1.36±0.05	1.41±0.07	1.48±0.07				1.38			
4	1.22±0.06	1.23±0.04	1.53±0.09	1.48±0.07	2.3±0.2		3.5±0.1	1.33	1.14		
5	1.09±0.03	1.21±0.04	1.49±0.09	1.35±0.07	2.1±0.2	2.4±0.1	3.4±0.1	1.16		1.5	
6	1.00	1.11±0.04	1.31±0.08	1.34±0.07						1.39	
7		1.00	1.19±0.06	1.27±0.06	1.8±0.2	2.3±0.1				1.28	
8			1.00	1.16±0.06	1.6±0.2	2.2±0.1					1.26
9				1.00	1.6±0.2	1.9±0.1					
10					1.4±0.2	1.8±0.1					
11					1.3±0.2	1.7±0.1					
12					1.1±0.2	1.5±0.1	2.8±0.1				
13					1.1±0.2	1.3±0.1	2.6±0.1				
14							2.0±0.1				
15							2.0±0.1				

[a]Reference [9].
[b]Reference [6].

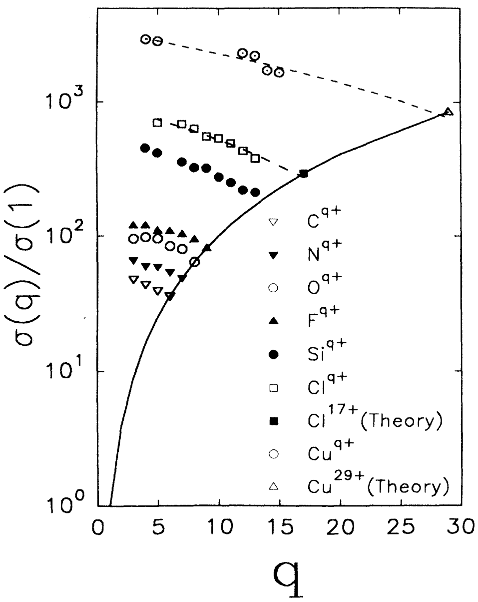

FIG. 3. Ratio of double-differential cross section for ions of charge state q relative to the double-differential cross section for protons on H_2. Cu projectile ions have an energy equal to 0.5 MeV/amu and all other ions have a beam energy of 1 MeV/amu. The solid line is the Z_p^2 prediction for $q = Z_p$, and the dashed lines are the best fit to the Cl and Cu data extrapolated to the bare ion for each case.

lower velocities [9]. In a separate paper [21] it was shown that, for C^{q+} $+H_2$ at the lower energy of 0.75 MeV/amu, the theory including the effects of the electron exchange is in much better agreement with the data than the theory not including exchange for all the charge states studied.

Figure 3 shows the ratio of the BEE DDCS for each projectile charge state studied to that calculated with the IA model for protons of the same energy per amu. The solid line is the Z_p^2 prediction for $q = Z_p$. The large enhancement of the DDCS as the charge state of the ion is decreased is seen clearly in this figure. The dashed lines are the best fit to the Cl and Cu data extrapolated to the bare ion for each case. The extrapolated ratios for Cl^{17+} and Cu^{29+} are 270±60 and 760±370, respectively, compared to the predicted Z_P^2 scaling ratios of 289 and 841, respectively. The IA predictions are represented in the figure by the solid square for Cl^{17+} and the up-triangle for Cu^{29+}. Miraglia and Macek [22] states that at 1.5 MeV/amu the Z_p^2 dependence is not strictly valid for $Z_p > 15$ within the continuum distorted wave–eikonal initial state and that higher orders in Z_p are needed. Data points for higher projectile charge states q are required to reduce the error bars in the extrapolation of the high-Z_p ratios to test this hypothesis.

B. BEE peak energy

In a classical two-body collision between a free electron and a projectile ion, the BEE peak (BEP) at an observation angle of 0° is expected to be independent of both q and Z_p and to have an energy of $4t$. Lee *et al.* [2] measured the BEP energy shift and found that it is about 94 eV for the F, O, N, and C ions at several projectile ion energies, and found it to be 37 eV for 1.5 MeV protons on H_2. Table II lists the energy shifts for the projectile ions studied in this work. For 1 MeV/amu H^+ ions the observed BEE peak, BEP, energy shift $\Delta E{=}4t - E_{\text{peak}}$ is approximately 68 eV in the laboratory frame, and for the light ions ($6 \leq Z_p \leq 9$) it is approximately 92 eV [see Fig. 4(a)]. In contrast, the BEP energy shift for the high Z_p projectile ions silicon, chlorine, and copper, showed a q dependence [see Figs. 2(b) and 4(b)–4(d)]. From Fig. 2(b) we see that, for the higher charge states, the peak is increasingly shifted toward lower energies. Figure 4 shows the BEP energy shift ΔE as a function of the projectile charge state q for (a) light ions (C, N, and O), (b) Si, (c) Cl, and (d) Cu. It is clear from this figure that the BEP energy shift for the high-Z_p projectile ions increases by increasing the charge state of the projectile. The energy shifts have been fitted to an equation of the

TABLE II. Experimental energy shifts $\Delta E{=}4t - E_{\text{peak}}$ in eV in the laboratory frame for 1 MeV/amu H, C, N, O, F, Si, and Cl, and 0.5 MeV/amu Cu projectile ions on H_2 as a function of the charge state of the projectiles. Theoretical energy shifts are calculated using the Bohr-Lindhard model [15].

q	H	C	N	O	F	SI	Cl	Cu	Theory
1	68								53
3		80±8	96±8	110±8					92
4		81±8	91±8	104±8		110±8		92±8	106
5		77±8	87±8	97±8		116±8	128±8	94±8	118
6		93±8	91±8	95±8					130
7			89±8	94±8		119±8	133±8		140
8				98±8		124±8	140±8		150
9					96±8	138±8	136±8		159
10						136±8	149±8		168
11						142±8	161±8		176
12						147±8	157±8	158±8	184
13						151±8	170±8	174±8	191
14								193±8	198
15								191±8	205

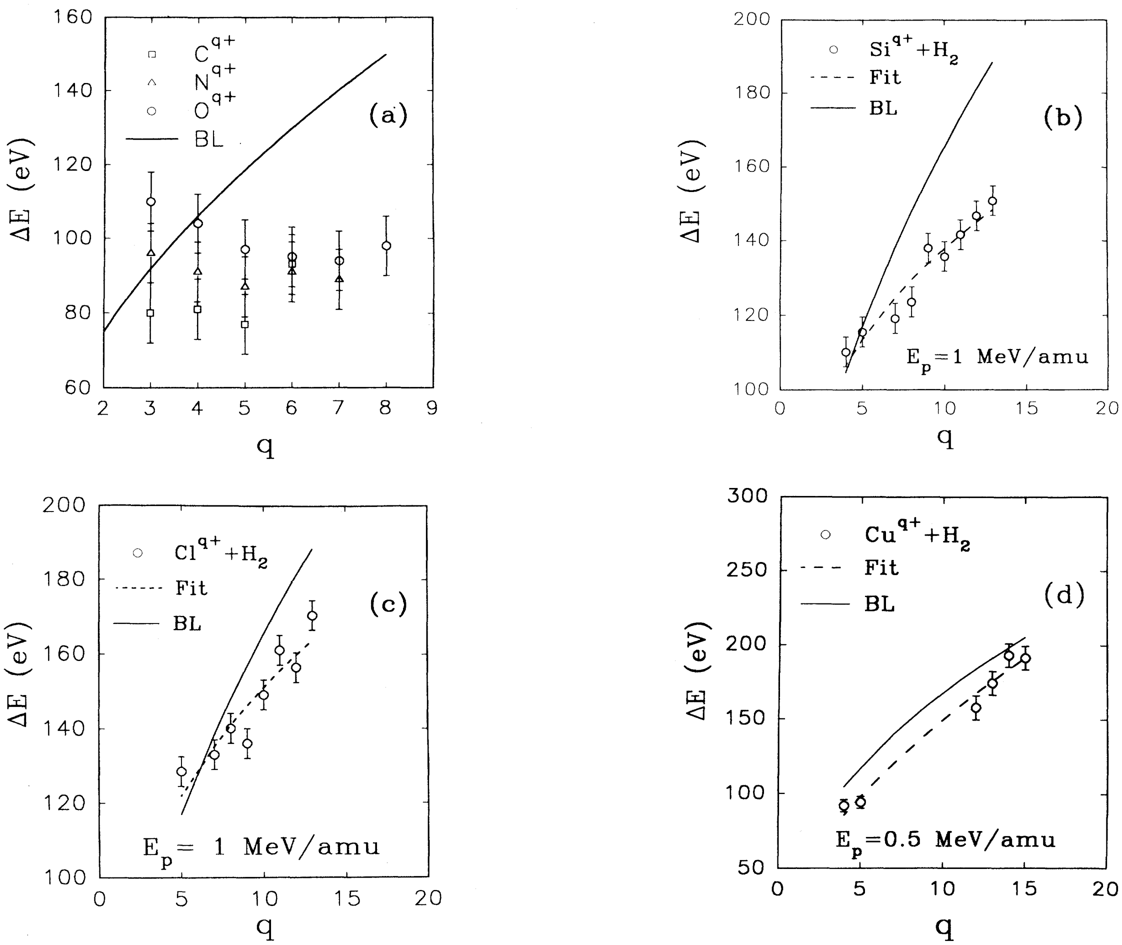

FIG. 4. Energy shifts $\Delta E = 4t - E_{\rm peak}$ (see text) as a function of the charge state q for 1 MeV/amu (a) C, N, and O, (b) Si, and (c) Cl projectile ions, and (d) for 0.5 MeV/amu Cu projectile ions. Circles, present data; dashed line, fit to the data, $\Delta E({\rm eV}) = aq^n$ with n and a given in Table III, solid line, Bohr-Lindhard (BL) model.

form $\Delta E = aq^n$. The fitting parameters are given in Table III. The best fit is indicated by the dashed lines in Figs. 4(b)–4(d).

Pederson *et al.* [15] give a prediction of the BEP energy shift, $\Delta E = 53\sqrt{q}$ eV, using the Bohr-Lindhard (BL) model, which is indicated in Fig. 4 by the solid lines and given in the last column of Table II. It appears from the data presented here that the slope of ΔE vs q approaches the prediction of the BL model as the nuclear charge of the projectile is increased. The best agreement is for the Cu^{q+} ions at 0.5 MeV/amu whereas all the other ions were at 1 MeV/amu. The observed shift can also be simulated from the IA model using Eqs. (3) and (4) by suitably adjusting the target ionization energy E_I. To obtain a larger BEP energy shift, E_I must be increased.

TABLE III. Fitting parameters of the experimental energy shift as a function of the charge state of the projectile using $\Delta E = aq^n$.

Parameter	Si	Cl	Cu
a (eV)	72±5	76±6	37±5
n	0.28±0.03	0.32±.08	0.61±0.06

An adiabatic resonant-tunneling model has been developed by Fainstein, Ponce, and Rivarola [23] which gives BEE peak shifts similar to the BL model.

The IA calculation used here predicts the shift to be about 88 eV and to be independent of the projectile nuclear charge Z_p and of the charge state q. For the low-Z_p projectiles we conclude that the shift is essentially independent of q [see Figs. 2(a), 4(a), and Table II]; however, for the high-Z_p projectile ions (Si^{q+}, Cl^{q+}, and Cu^{q+}), the data clearly indicate that the energy shift is dependent on q [see Figs. 4(b)–(d)].

Figure 5 shows the energy shift ΔE of the bare ions as a function of Z_p. The Si, Cl, and Cu bare projectile ions could not be obtained with sufficient numbers using the available accelerator. The data in Fig. 4 were extrapolated using the results of the best fits to the data to get the energy shifts for these bare ions. It is clear from this figure that the energy shift is Z_p dependent. The dashed line in Fig. 5 is the Bohr-Lindhard prediction $\Delta E = 53\sqrt{Z_p}$ eV [15] and the solid line is the IA prediction for the BEE energy shift for E_I =15.5 eV. Miraglia and Macek [22] calculated this energy shift in different approximations. Their calculation given only for

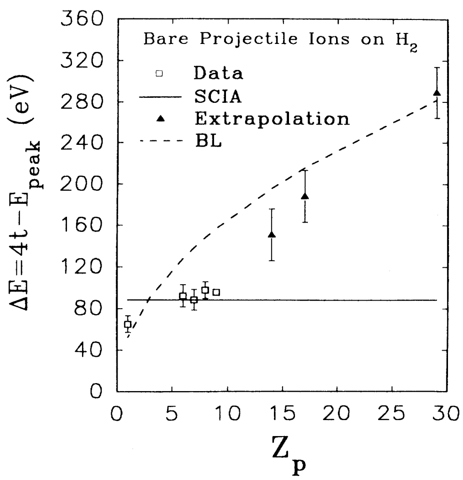

FIG. 5. Energy shifts ΔE (see text) as a function of projectile nuclear charge Z_p. Squares, present data; triangle; extrapolation from the fit in Fig. 4; solid line, calculation according to the semiclassical impulse approximation (SCIA); dashed line, Bohr-Lindhard (BL) model.

Z_p=9 underestimates the magnitude of ΔE by about 50 eV whereas the Bohr-Lindhard calculation overestimates the shift near Z_p=9 by about 60 eV.

V. CONCLUSIONS

In summary, the charge-state dependence of the binary-encounter electron double-differential cross section at 0° in the laboratory frame has been studied for both low-Z_p projectiles ($Z_p \leq 9$) as well as high-Z_p projectiles (Z_p=14, 17, and 29). The data showed that the BEE DDCS increases with increasing number of electrons on the projectile for all projectiles studied. The impulse approximation calculation for the BEE process also predicts an enhancement of the cross section with increasing q when the static potential of the non-bare projectile ion and the electron-electron exchange are included. No IA calculations are available in the literature at the present time for Si, Cl, and Cu.

The IA calculations using the Hartree-Fock model for the electron-ion scattering as presented for C^{q+} [21] predicts the BEE peak position to be independent of the charge state . This model is consistent with the data for low-Z_p projectiles ($Z_p \leq 9$) which exhibit no BEE peak shift within the measured uncertainties. The IA calculations will presumably show no q-dependent energy shift for high-Z_p projectiles. The data presented here for Si, Cl, and Cu showed that the BEP energy shift ΔE is dependent on the projectile charge state. An *ad hoc* estimate of the energy shift using the Bohr-Lindhard model [15] in which the target electron has a release radius given by the condition that the electrostatic target and projectile forces on the electron are equal shows a q dependence of the BEP energy shift. This model does not agree very well with the observed energy shifts. For low-Z_p projectiles it predicts an energy shift where no shift is observed within the error of the experiment (e.g., 92 eV for O^{3+} and 150 eV for O^{8+} compared to measured values of 110±8 eV and 98±8 eV, respectively). The BL model prediction appears to improve as the projectile nuclear charge increases. In order to predict ΔE for all the data, a model which predicts a different q dependence as a function of Z_p must be found.

ACKNOWLEDGMENTS

We would like to acknowledge stimulating discussions with R. Shingal and C. P. Bhalla. This work was supported by the Division of Chemical Sciences, Office of Basic Energy Sciences, Office of Energy Research, U.S. Department of Energy. One of us (T.J.M.Z.) would like to acknowledge the support of NATO collaborative research Grant No. CRG-910567.

[1] N. Stolterfoht, in *Structure of Collisions of Ions and Atoms,* edited by I.A. Sellin (Springer-Verlag, Berlin, 1978), p. 155.
[2] D.H. Lee, P. Richard, T.J.M. Zouros, J.M. Sanders, J.L. Shinpaugh, and H. Hidmi, Phys. Rev. A **41**, 4816 (1990).
[3] P. Richard, D.H. Lee, T.J.M Zouros, J.M. Sanders, and J.L. Shinpaugh, J. Phys. B **23**, L213 (1990).
[4] C. Kelbch, R.E. Olson, S. Schmidt, H. Schmidt-Böcking, and S. Hagmann, J. Phys. B **22**, 2171 (1989).
[5] S. Hagmann, W. Wolff, J.L. Shinpaugh, H.E. Wolf, R.E. Olson, C.P. Bhalla, R. Shingal, C. Kelbch, R. Herrmann, O. Jagutzki, R. Dörner, R. Koch, J. Euler, U. Ramm, S. Lencinas, V. Dangendorf, M. Unverzagt, R. Mann, P. Mokler, J. Ullrich, H. Schmidt-Böcking, and C.L. Cocke, J. Phys. B **25**, L287 (1992).
[6] D.R. Schultz and R.E. Olson, J. Phys. B **24**, 3409 (1991).
[7] R. Shingal, Z. Chen, K.R. Karim, C.D. Lin, and C.P. Bhalla, J. Phys. B **23**, L637 (1990).
[8] Z. Chen, Don Madison, and C.D. Lin, J. Phys B **24**, 3203 (1991).
[9] C.P. Bhalla and R. Shingal, J. Phys B **24**, 3187 (1991).
[10] C.O. Reinhold, D.R. Schultz, and R.E. Olson, J. Phys. B **23**, L591 (1990).
[11] K. Taulbjerg, J. Phys. B **23**, L761 (1990).
[12] A.D. González, P. Hvelplund, A.G. Peterson, and K. Taulbjerg, J. Phys. B **25**, 157 (1992).
[13] P. Hvelplund, H. Tawara, K. Komaki, Y. Yamazaki, K. Kuroki, H. Watanabe, K. Kawatsura, M. Sataka, M. Imai, Y. Kanai, T. Kambara, and Y. Awaya, J. Phys. Soc. Jpn. **60**, 3675 (1990).
[14] O. Jagutzki, S. Hagmann, H. Schmidt-Böcking, R.E. Olson, D.R. Schultz, R. Dörner, R. Koch, A. Skutlartz, A. González, T. B. Quinteros, C. Kelbch, and P. Richard, J. Phys. B **24**, 2579 (1991).

[15] J.O. Pederson, P. Hvelplund, A.G. Petersen, and P.D. Fainstein, J. Phys. B **24**, 4001 (1991).
[16] D.H. Lee, T.J.M. Zouros, J.M. Sanders, J.L. Shinpaugh, T.N. Tipping, S.L. Varghese, B.D. DePaola, and P. Richard, Nucl. Instrum. Methods Phys. Res. B **40/41**, 1229 (1989).
[17] D. Brandt, Phys. Rev. A **27**, 1314 (1983).
[18] F. Drepper and J.S. Briggs, J. Phys. B **9**, 2063 (1976).
[19] J.M. Sanders (private communication).
[20] The enhancement ratios for Si, Cl, and Cu were evaluated by taking the ratio of the measured $\sigma(q)$ to $\sigma(Z_p)$ calculated from the IA with an E_I value that best predicts the BEE peak position.
[21] H.I. Hidmi, C.P. Bhalla, S.R. Grabbe, J.M. Sanders, P. Richard, and R. Shingal, Phys. Rev. A **47**, 2398 (1993).
[22] J.E. Miraglia and J. Macek, Phys. Rev. A **43**, 5919 (1990).
[23] P.D. Fainstein, V.H. Ponce, and R.D. Rivarola, Phys. Rev. A, **45** 6417 (1992).